THE JOURNAL OF PHYSICAL CHEMISTRY A

pubs.acs.org/JPCA

Article

Noncommutative Switching of Double Spiropyrans

Luuk Kortekaas, Jorn D. Steen, Daniël R. Duijnstee, Denis Jacquemin,* and Wesley R. Browne*

Cite This: J. Phys. Chem. A 2020, 124, 6458−6467

Read Online

ACCESS | Metrics & More | Article Recommendations | Supporting Information

ABSTRACT: The spiropyran family of photochromes are key components in molecular-based responsive materials and devices, e.g., as multiphotochromes, covalently coupled dyads, triads, etc. This attention is in no small part due to the change in properties that accompany the switch between spiropyran and merocyanine forms. Although the spiropyran is a single structural isomer, the merocyanine form represents a family of isomers (*TTT*, *TTC*, *CCT*, etc.) and protonation states. Combining two spiropyrans into one compound increases the number of possible structures dramatically and the interaction between the units determines, which are impeded due to intramolecular quenching of excited states. Here, we show that the coupling of two spiropyran photochromes through their phenol units yields favorable interactions (crosstalk) between the components that provides access to species inaccessible with the component monospiropyran alone. Specifically, the ring opening of one spiropyran unit, which is thermally stable at −30 °C, prevents ring opening of the second spiropyran unit. Furthermore, whereas protonated *E*- and *Z*-monomerocyanines were previously shown to undergo thermal- and photo-equilibration, the corresponding protonated *E*- and *Z*- bimerocyanines are thermally stable and show one-way photoisomerization from the *Z*,*Z*- to an emissive *E*,*E*-bimerocyanine form. Subsequent deprotonation at room temperature resets the system to the bispiro ring-closed form, but deprotonation at −30 °C yields the otherwise inaccessible bimerocyanine form. This form is photochemically inert but undergoes a two-step thermal relaxation via the merocyanine-spiropyran form, showing that the connection at the phenol units provides sufficient intramolecular interaction to fine-tune the complex isomerization pathways of spiropyrans and demonstrating noncommutability in photo- and pH-regulated multistep isomerization pathways.

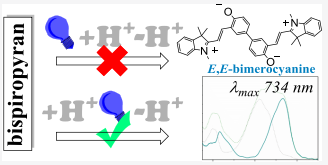

INTRODUCTION

Molecular switches are instrumental in creating functional materials, through enabling reversible changes in macroscopic properties with external stimuli such as irradiation,[1] heat,[2,3] electricity,[4] and pH.[5] Of the wide range of stimuli-responsive compounds, photochromic dithienylethenes,[6] azobenzenes,[7,8] and spiropyrans[9,10] in many different forms are the most prominent members. The synthetic flexibility and diversity of these photochromic building blocks have enabled fine-tuning of their (photo)physical properties, tailoring the properties of smart materials. The rational integration of molecular switches and devices benefits greatly when the effect of changes in the molecular structure on their photochemistry is predictable.

The spiropyran photochromes are particularly attractive due to their synthetic and functional flexibility[9−14] and are key components in multicomponent systems.[15−19] They enable control of material properties[9,19] due to the large change in molecular structure and properties (dipole moment, charge) upon switching between their spiropyran and merocyanine forms (Scheme 1) induced by a wide range of stimuli, e.g., light, heat, pH changes, etc.[10] Furthermore, the "merocyanine form" is itself a family of distinct structures, each with their own properties and reactivity (Scheme 1).

The photochemical ring opening of the spiro unit generates a merocyanine form either as a *Z*- (i.e., *CCC*, *CCT*, *TCC*, and *TCT*) or an *E*-isomer (i.e., *TTT*, *TTC*, *CTT*, and *CTC*). The deprotonated *Z*-isomer is formed only transiently due to the large driving force for ring-closing and is observed only at low temperature[24] or by transient spectroscopy.[9,25−28] For the *E*-isomer, several transoid merocyanine conformational isomers are possible with respect to the configuration about the α, β, and γ bonds (gray box in Scheme 1) in the pyran alkene bridge. The *TTC* form is generally regarded as the most thermodynamically stable of the *E*-isomers,[29] usually followed closely by the *TTT* form. The stability of the *TTC*-isomer is ascribed to H-bonding of the phenolate with the C3′−H hydrogen (Scheme 1).[20−22] However, other isomers have been observed by transient spectroscopy, including those of the nonsubstituted monospiropyran (**1**, Scheme 2) studied here.[30] Protonation stabilizes both the *Z*- and *E*-merocyanine isomers of **1**, which interconvert reversibly upon irradiation at 365 and 455 nm, respectively.[23] Calculations indicate that the protonated *E*-isomer adopts the *TTT*-conformation preferentially, which is consistent with the absence of stabilization by C3′−H/phenolate H-bonding (Scheme 1).[20−22]

Isomerization dynamics following excitation of the *transoid* merocyanines have been well studied in particular for those

Received: March 15, 2020
Revised: July 19, 2020
Published: July 21, 2020

https://dx.doi.org/10.1021/acs.jpca.0c02286
J. Phys. Chem. A 2020, 124, 6458−6467

Scheme 1. Photochemical Conversion of the Ring-Closed Spiropyran to the Ring-Open Merocyanine Form Is Thermally Reversible[a]

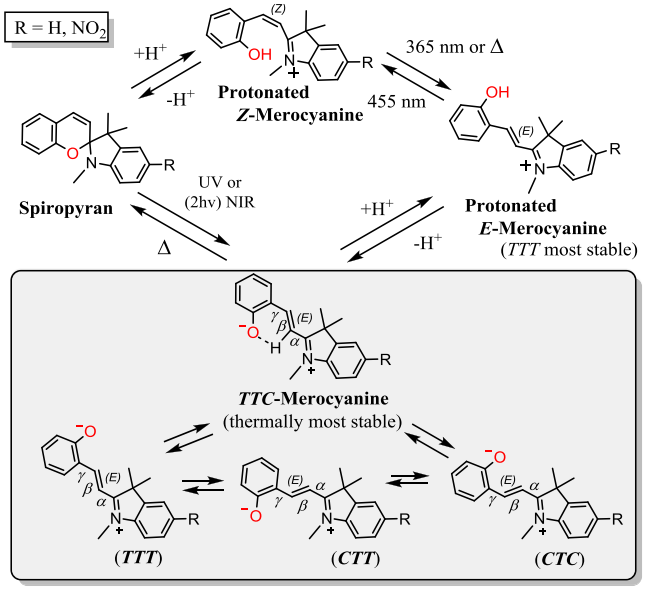

[a]Protonation of either form inhibits ring-closing, and reversible *Z*/*E*-isomerization is observed instead. In the nonprotonated form, *TTC*-merocyanine is generally most stable due to H-bonding;[20−22] however, this interaction is lost upon protonation and the *TTT* form becomes energetically most favored.[23] The "C" and "T" in the three-letter abbreviations indicate *cis*(oid) or *trans*(oid) configuration about the α, β, and γ positions, with *Z*- (i.e., C) and *E*-isomers (i.e., T) indicating configuration at the β-position.

Scheme 2. Spiropyrans 1, 2, and 3[a]

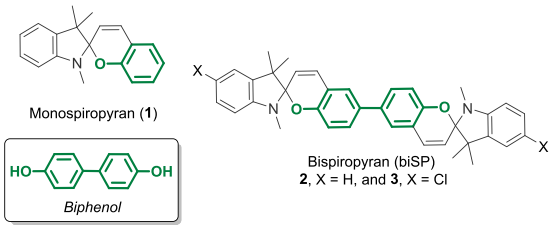

[a]The coupling of spiropyran photochromes via the pyran unit forms a biphenol central motif.

with electron-withdrawing substituents at both the 6- and 8-position (ortho and para to the phenol unit), e.g., 6,8-dinitrobenzoindolinospiropyran and 6-nitro-8-bromobenzoindolinospiropyran, as the merocyanine form can thus be tuned to be thermally preferred in polar solvents.[21,22,31−33] The *TTC* form is the dominant species in thermal equilibrium with minor amounts of the *TTT* form present. Although 6-nitrobenzoindolinospiropyrans are stable only in the ring-closed spiro form, the formation of the *TTC*- as well as the *TTT*-isomer upon photoexcitation was inferred from their distinct emission spectra upon excitation at >610 nm, and the *TTT*-isomer was confirmed as a transient form by femtosecond transient absorption spectroscopy.[34] Notably, while some reports propose *TTC* to *TTT* and *TTT* to *TTC* interconversion upon excitation of the substituted merocyanines as a minor photochemical pathway, Brixner and co-workers later reported that photochemical switching was essentially one way, i.e., the *TTC* to *TTT* photoconversion is photochemically irreversible.[35] It should be noted that the assignments of structure (*TTC*, *TTT*, etc.) in the ultrafast studies rely heavily on theoretical studies. However, this uncertainty does not affect the broader conclusions reached, in that the observation of these species on the ground-state surface coupled to theoretical studies is certainly useful in building a more solid basis for interpretation, especially in more complex multicomponent structures.

Although understanding simple representative compounds such as **1** is an essential first step in understanding more complex molecular systems, multicomponent molecular-based systems such as the double spiropyrans **2** and **3** (in which the two spiropyran (**1**) units are coupled directly through their pyran moiety to form a biphenyl bridge, Scheme 2) can present unexpected complexity in their operation. The functionality of each unit in multicomponent systems[14,19,36−41] can be affected negatively by crosstalk (interference) between the units or can cause the emergence of new and unexpected functionalities.[36,41]

In the present report, we show how these more complex systems provide detailed insight into the fundamental photo- and thermochemistry of spiropyrans. We show that the biphenol moiety in **2** and **3** provides sufficient interaction between the spiropyran units to enable the generation of *E*,*E*-isomers only through a series of noncommuting pH-jumping and photochemical operations as follows (Scheme 3). At room

Scheme 3. Noncommutative Operations Leading to the Formation of *E*,*E*-Isomer through pH-Gating (Light-Blue Arrows)

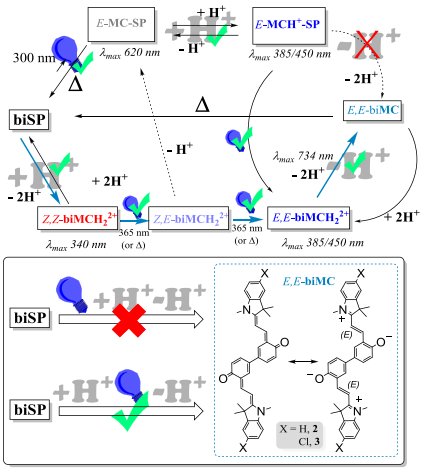

temperature, the photochemically generated spiropyran-merocyanine (SP-[*E*-MC]) isomers of **2** and **3** exhibit rapid thermal reversion to their bispiropyran (biSP) form. In contrast, the addition of strong acid (CF_3SO_3H) generates the thermally stable protonated *Z*,*Z*-bimerocyanine isomer (*Z*,*Z*-biMCH$_2^{2+}$), which undergoes one-way conversion to the stable protonated *Z*,*E*-isomer (*Z*,*E*-biMCH$_2^{2+}$) and then *E*,*E*-isomer (*E*,*E*-biMCH$_2^{2+}$) photochemically as well as thermally (indicating that the *E*-forms are thermodynamically more stable).

The photochemical and thermal irreversibility of the *Z*/*E*-isomerization in the protonated forms is in contrast to **1**, in which *Z*/*E*-isomerization is reversible under protonating conditions.[23] Unexpectedly, deprotonation of the *E*,*E*-biMCH$_2^{2+}$ form provides transient access to the deprotonated

https://dx.doi.org/10.1021/acs.jpca.0c02286
J. Phys. Chem. A 2020, 124, 6458−6467

Scheme 4. Synthesis of Bispiropyrans 2 and 3

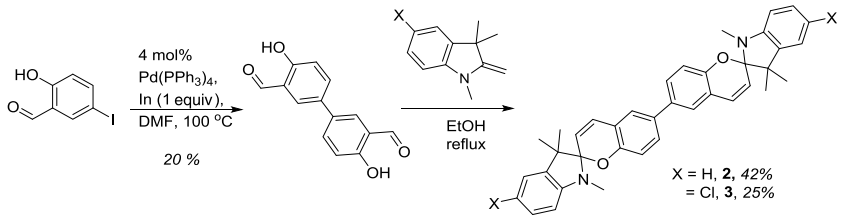

E,E-merocyanine isomer also, rather than essentially exclusive formation of the singly opened SP-[*E*-MC]-form (Spiropyran-merocyanine) that is obtained by direct irradiation of bispiropyran at low temperatures.[20] The noncommutative behavior demonstrates that the interaction between units in the double spiropyrans depends critically on the protonation state. The characterization of the *Z,E*- and *E,E*-merocyanine isomers by steady-state spectroscopies provides the essential insight necessary for tuning the thermal and excited state dynamics of spiropyrans.

EXPERIMENTAL SECTION

Synthetic Procedures and Materials. **2** and **3** were prepared in the present study by aryl homo-coupling with a palladium/indium bimetallic catalyst as described by Chang et al.[42] followed by double Fischer base condensation to the respective indolines (Scheme 4 and Supporting Information), and characterization was consistent with earlier reports.[42−46] All chemicals for the synthesis of **2** and **3** were purchased from Aldrich or TCI and were used without further purification. High-performance liquid chromatography (HPLC) grade acetonitrile was used without additional purification for spectroscopic measurements.

Methods. ^{1}H, ^{13}C attached proton test (APT) and distortionless enhancement by polarization transfer (DEPT), heteronuclear single quantum coherence (HSQC), and heteronuclear multiple bond correlation nuclear magnetic resonance (HMBC NMR) spectra were obtained on a Bruker 600 spectrometer. In situ photochemical switching was followed by NMR spectroscopy (Bruker 500 spectrometer) with the irradiation by fiber-coupled diodes (vide infra) with ca. 3 cm of the end of the fiber declad and abraded to allow for emission along the length of the sample. Chemical shifts (δ) are reported in parts per million with respect to tetramethylsilane and referenced to residual solvent (CHD_2CN) signals, and coupling constants in Hertz. Multiplicities are denoted as: s = singlet, d = doublet, t = triplet, br = broad singlet, m = multiplet. Fourier transform infrared (FTIR) spectra were recorded on a PerkinElmer Spectrum400 FTIR spectrometer. Electrospray ionization-mass spectrometry (ESI-MS) was recorded on an LTQ Orbtitrap XL spectrometer. UV−vis absorption spectra were recorded on an Analytik Jena Specord600 spectrometer. Irradiation at 300 (370 μW), 365 (4.1 mW), 455 (3.2 W), 490 (2.3 mW), 565 (2.0 mW), and 660 nm (14.5 mW) was provided by diodes (M300F2, M365F1, M455L3-C5, M490F1, M565F1, and M660F1, respectively, from Thorlabs). UV−vis absorption spectra were recorded at −30 °C using a Quantum Northwest temperature-controlled cuvette holder. Absolute quantum yields were determined as described earlier,[23] using the ferrioxalate-based actinometric method described by Hatchard and Parker.[47] Emission spectra at −30 °C were obtained by excitation with the aforementioned laser diodes, with a 500 nm short-pass filter in front of the M490F1 LED light source specifically in the case of the fluorescence of *E*-biMCH$_2^{2+}$. Room temperature emission spectra were obtained by excitation at 490 nm (LED M490F1, Thorlabs) at 90° to the collection axis with emitted light collected by a pair of 25 mm diameter planoconvex lenses (f = 7.5 cm) and fed via a long-pass filter into a Shamrock500i spectrograph onto a iDus-420-BU CCD detector.

Density Functional Theory (DFT) Calculations. All our theoretical calculations have been performed with the Gaussian16.A03 code,[48] using default approaches, algorithms, and thresholds, except when noted below. We have followed a computational protocol similar to the one proposed by Bieske[49] and applied in our previous work as well.[23] We performed DFT geometry optimization and vibrational frequency calculations with the PW6B95D3 functional combined with the def2-TZVP atomic basis sets. We accounted for solvent effects systematically using the polarizable continuum model. For determining various transition states, we followed exactly the same protocol as in our previous work;[23] that is, we computed the Hessian at each step, starting from structures build by linking two "mono minima/TS" taken from ref 23 as a starting point. Note that, as previously, the BS-DFT wavefunction collapsed into the restricted solution and the latter approach is applied here. TD-DFT calculations were performed with the CAM-B3LYP functional[50] and *aug*-cc-pVDZ, using the vertical approximation.

RESULTS AND DISCUSSION

The presence of the chloro-substituent in **3** facilitated studies by ^{1}H NMR spectroscopy (vide infra). Details and characterization by ESI-QMS, one-dimensional (1D) and two-dimensional (2D) ^{1}H NMR, UV−vis absorption, and FTIR spectroscopy (Figure S1) can be found in the Supporting Information.

Photochromism of Bispiropyrans. The UV−vis absorption spectra of bispiropyrans **2** and **3** show absorption in the UV region, typical of spiropyrans. Irradiation with UV light at room temperature results in only a minor transient increase in visible absorption (Figure S2), consistent with a low thermal barrier to a reversion of the merocyanine forms to the original spiropyran form (Figure 1); the calculated barriers for thermal interconversion between the SP, the thermodynamically unstable *CCC*, *TTT*, and *TTC* forms are at most 20 kcal mol^{-1} (Figure 1 and Scheme S1). The *TTC* form is calculated to be only marginally less stable than the *TTT* form, indicating that both species should be present.

At −30 °C, photoinduced ring opening proceeds for both **2** and **3** (Figures 1 and S2), with absorption maxima at 395 and 619 nm and shoulders at 408 and 660 nm. An additional weak band at ca. 750 nm also appears, which is ascribed to a second species (Figure S2, vide infra). The visible absorption is shifted bathochromically compared to monospiropyran **1** (λ_{max} 385

https://dx.doi.org/10.1021/acs.jpca.0c02286
J. Phys. Chem. A 2020, 124, 6458−6467

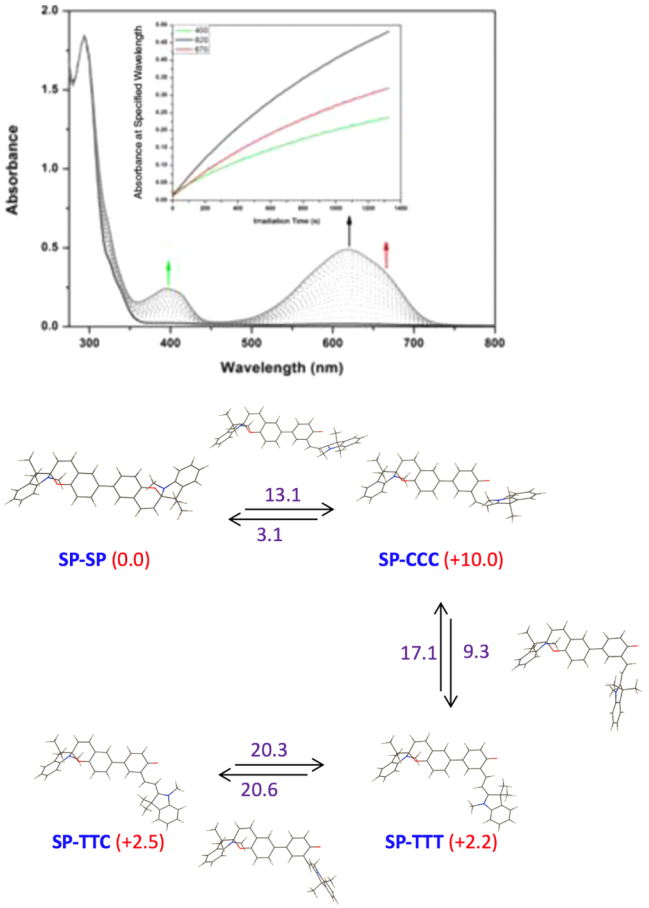

Figure 1. (Top) UV−vis absorption spectroscopy of **2** (88 μM in acetonitrile) during 300 nm irradiation at −30 °C, inducing ring opening of the colorless biSP form (black line) to the colored SP-[*E*-MC] form (gray line). (Bottom) DFT relative energies relative to biSP and barriers (kcal mol^{-1}) for thermal isomerization of one spiropyran unit of **2** at room temperature. Transition state structures are shown above arrows. The *CTC* and *CTT* isomers were not located[23] as stable structures in the monomeric species and were not further investigated. The barriers for the conversion of the second SP unit can be found in Scheme S1.

and 582 nm with a shoulder at 398 nm), and, notably, the molar absorptivity (if full conversion is assumed) is ca. 6000 M^{-1} cm^{-1}, indicating that the photostationary state reached is low. However, the photochemical quantum yields in both cases, 6%, are similar to those of the indolinobenzospiropyrans (i.e., **1**, ca. 7%),[23] and, as with **1**,[51] visible light does not induce photoreversion. Hence, the low molar absorptivity cannot be due to reaching a photostationary state in which there is a mixture of SP-SP, *E*-MC-SP, and *E*,*E*-biMC but instead reflects the switching of only one of the two spiropyran units (vide infra).

Acidochromism of Bispiropyrans. The acidochromism of spiropyrans is well known,[9,52−62] and recently we reported that strong acids (i.e., those with a pK_a lower than that of the *E*- and *Z*- merocyanine forms) induce spontaneous ring opening of spiropyrans to their *Z*-merocyanine form.[23] Irradiation with UV light induces *Z*- to *E*-isomerization of the protonated merocyanine. For monospiropyrans, such as **1**, *Z*- to *E*-isomerization is reversed upon irradiation with visible light.

For the double bispiropyrans **2** and **3**, addition of stoichiometric CF_3SO_3H induces spontaneous ring opening to the protonated *Z*-bimerocyanine form manifested by an increase in absorbance at 341 nm (Figures 2) and a complete change in the ^{1}H NMR spectra (vide infra, Figure S12). Stepwise addition of substoichiometric amounts of acid results in a steady and stepwise change in absorbance without evidence for intermediate species even at −30 °C (Figure S4). By contrast, the stepwise addition of CF_3SO_3H reveals intermediate protonated species by ^{1}H NMR spectroscopy (Figure S13). These data indicate that a thermally stable intermediate can be formed upon partial protonation, most probably the singly protonated [*Z*-MCH$^+$][SP] species, with several signals of the remaining spiropyran unit shifting by a few fractions of a ppm as a result. Furthermore, the chemical shifts of the protonated [*Z*-MCH$^+$] unit of the mixed [*Z*-MCH$^+$][SP] species are substantially different from those of the fully open *Z*,*Z*-biMCH$_2^{2+}$ forms, indicating that the rate of ring opening and closing between the [*Z*-MCH$^+$] and SP states is longer than the NMR timescale, (ca. 10 ms) and therefore controlled by the rate of proton transfer.

Subsequent deprotonation recovers the UV−vis absorption and ^{1}H NMR spectra of the spiropyran form (Figures S3 and S12). These data further indicate that the communication between the spiropyran units is limited and protonation of both moieties proceeds statistically. Indeed, the calculated stabilities of the various species (spiro and protonated merocyanine) support this analysis (Scheme S2).

pH-Gated Photochromism of Bispiropyrans. Irradiation of the protonated *Z*-bimerocyanines at 365 nm results in the appearance of absorption bands at 385 and 450 nm with an isosbestic point maintained at 350 nm, suggesting *Z*/*E*-isomerization proceeds without significant steady-state concentrations of intermediates (Figure 2). However, ^{1}H NMR spectroscopy (vide infra) shows clearly that the isomerization indeed proceeds in a stepwise manner at each of the merocyanine units, with the formation of a [*Z*-MCH$^+$]−[*E*-MCH$^+$] species. The UV−vis absorption bands are red-shifted compared to the single band at 420 nm observed for the corresponding monospiropyran **1**;[23] however, this may reflect inductive effects rather than stabilization of the lowest unoccupied molecular orbital (LUMO) by forming a cyanine structure. The photochemical quantum yield of 91% is similar to that (92%) of **1**.[23]

An intermediate species was observed by ^{1}H NMR spectroscopy upon in situ irradiation at 365 nm of protonated **2** (*Z*,*Z*-biMCH$_2^{2+}$ form) (Figure S14), supporting the conclusion that there are several accessible isomers in the protonated merocyanine form. Eventually, the energetically most favored state dominates, which is assigned to a mixture of the *TTC* and *TTT* isomers in rapid equilibrium in accordance with the low barrier to isomerization (theory indicates a ca. 0.1 ms, which is faster than the NMR timescale). The additional intermediate signals observed are most likely due to differences between the mixed Z/E intermediates and the fully switched *E*,*E*-biMCH$_2^{2+}$ form.

In contrast to monospiropyrans, the protonated *Z*- and *E*-isomers do not show appreciable thermally induced interconversion at room temperature, nor does irradiation at 455 nm induce reversion of the *E*-form to the *Z*-form. This behavior is consistent with the calculated relative stability of the *E*-forms and the large barrier to *E*−*Z* isomerization (>30 kcal mol^{-1}, Scheme 5).

https://dx.doi.org/10.1021/acs.jpca.0c02286
J. Phys. Chem. A 2020, 124, 6458−6467

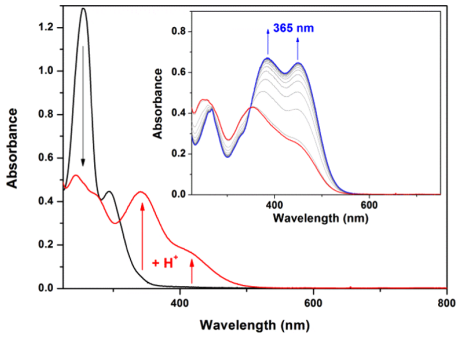

	2	3
biSP	$_{295nm}$ = 21500 M^{-1} cm^{-1}	$_{294nm}$ = 17200 M^{-1} cm^{-1}
Z,Z-MCH_2^{2+}	$_{338nm}$ = 20300 M^{-1} cm^{-1}	$_{341nm}$ = 17050 M^{-1} cm^{-1}
E,E-MCH_2^{2+}	$_{377nm}$ = 30100 M^{-1} cm^{-1}	$_{385nm}$ = 25650 M^{-1} cm^{-1}

Figure 2. (Top) UV−vis absorption spectrum of **3** (26 μM in acetonitrile) upon addition of 2.5 equiv CF_3SO_3H to form the *Z,Z*-biMCH$_2^{2+}$ form and (inset) subsequent irradiation at 365 nm to form the *E,E*-biMCH$_2^{2+}$ form (note that with weaker acids, such as CF_3CO_2H, the extent of ring opening is limited, Figure S4). (Bottom) Molar absorption coefficients of the ring-closed biSP and protonated open forms.

Scheme 5. Intermediate Protonation State of Bispiropyrans Observed by ^{1}H NMR Spectroscopy

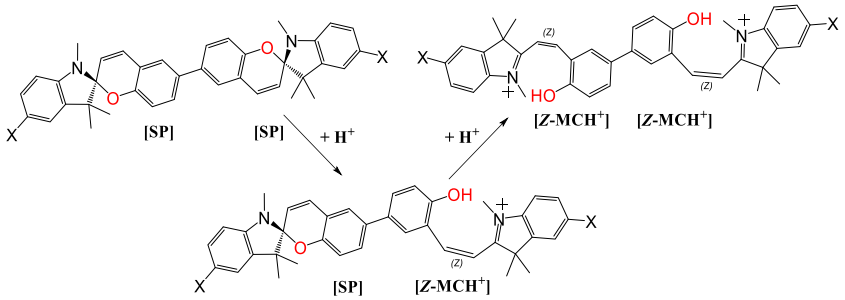

In summary, protonation results in the formation of a thermally stable open isomer *Z,Z*-biMCH$_2^{2+}$ at room temperature and the thermally stable isomer *E,E*-biMCH$_2^{2+}$ is formed irreversibly upon irradiation with UV light (Figure S5).

Deprotonation of the *E,E*-biMCH$_2^{2+}$ form of **2** or **3** with Et_3N or sodium acetate recovers the merocyanine state (Figure 3 and Figure S6).[23] However, in contrast to the visible absorption spectrum obtained by irradiation of **2** or **3** at −30 °C (vide supra, Figure 1), generation of the deprotonated merocyanine form by addition of base to *E,E*-biMCH$_2^{2+}$ results in an additional absorption band at 734 nm (Figure S6), which is assigned to the *E,E*-biMC isomer (vide infra). Assignment of the 734 nm band to aggregation, observed for spiropyrans earlier,[9,63] can be excluded as the shape of the absorption spectrum is independent of concentration (Figure S7), even as low as 3 μM. Stepwise addition of base results in an increase in near-IR absorption bands with a slight delay, indicating that the *E,E*-biMC isomer is less acidic than the SP-[*E*-MC] isomer (Figure S8).

The assignment of the species absorbing at 730 nm to the TTC form of *E,E*-biMC and not the formation of other isomers is supported by DFT calculations. TD-CAM-B3LYP calculations yield vertical absorptions at 528 and 551 nm for the *TTC* and *TTT* forms, respectively. The fact that the values are hypsochromically shifted, compared to the measured spectra, is due to the use of the vertical approximation. The absorption of the *TTT* form is red-shifted compared to the *TTC* form, which is consistent with that proposed for monomerocyanines from transient absorption studies.[29,31,32,35,64] These data are consistent, in terms of order, with the small differences in ground-state energies but not with the magnitude of the experimentally obtained shift in absorption maximum. Both of the merocyanine isomers obtained following deprotonation of *E,E*-biMCH$_2^{2+}$ are relatively stable at −30 °C, although the absorption band in the NIR (734 nm) decays more rapidly than the absorption band at 620 nm upon heating (Figure 4), which is consistent with the lower thermal barrier for *E,E*-biMC to *E*-MC-SP than from *E*-MC-SP to SP-SP. The spectra obtained upon full deprotonation, i.e., containing both bimerocyanine and spiropyran-merocyanine isomers, are unaffected by further irradiation at 365, 565, or 660 nm, which is in line with the lack of photoreactivity in merocyanines that do not bear electron-withdrawing substituents. Notably, photochemical *TTC*−*TTT* interconversion in dinitro-substituted monospiropyrans was observed as only a negligible pathway in ultrafast spectroscopy also,[65,66] with only efficient unidirectional *TTC* to *TTT* isomerization observed.[34,35]

Neither the closed bispiropyran form (λ_{exc} 300 nm) nor the *Z,Z*-biMCH$_2^{2+}$ form (λ_{exc} 365 or 420 nm) show fluorescence, which is consistent with rapid excited state quenching due to the isomerization channels available.[26,67] Similarly although they do not show photoactivity, the nonprotonated *E,E*-biMC forms (λ_{abs} 619 or 734 nm) do not show fluorescence either

https://dx.doi.org/10.1021/acs.jpca.0c02286
J. Phys. Chem. A 2020, 124, 6458−6467

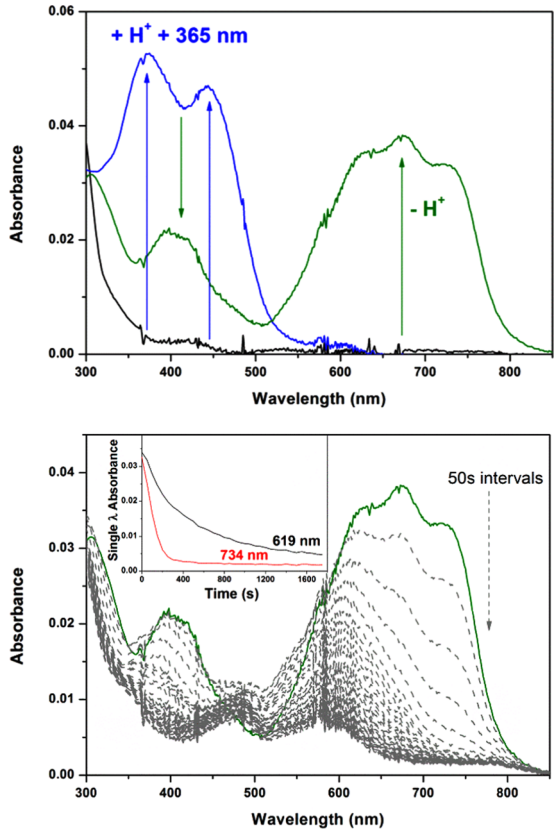

Figure 3. (Top) UV−vis absorption spectra of **2** (2.0 μM in acetonitrile) at −30 °C, before (black line) and after protonation with 6 equiv of CF_3SO_3H and subsequent irradiation at 365 nm (blue line), followed by deprotonation with excess (75 equiv) of NaOAc in 9:1 acetonitrile/water (green line). (bottom) Decay of the bimerocyanine and spiropyran-merocyanine isomers generated by deprotonation at −30 °C (at 50 s intervals).

(at λ_{exc} 565, 660 or 691 nm) at −30 °C, indicating that the lack of photochemical switching is likely due to a rapid nonreactive decay channel from the excited state, i.e., an easily accessible conical intersection.

Although the protonated monomerocyanines show photoinduced *E*/*Z* isomerization and do not show significant fluorescence either,[23] the thermodynamically stable protonated bimerocyanines (*E*-biMCH$_2^{2+}$ forms of **2** and **3**) show fluorescence (Figures S10 and S11). This contrast between the mono- and bispiropyran underlines the ability of the bimerocyanine units to communicate electronically to the extent that new functionality emerges.

pH-Gated ^{1}H NMR Spectroscopy of Bispiropyrans. As with indolinobenzospiropyrans,[23] the stability of the accessible protonated bimerocyanine forms allows for their observation by ^{1}H NMR spectroscopy. For **2**, the chemical shifts and changes in coupling constants for the alkene bridge and alkyl methyl substituents are essentially identical to those of the thermally most stable *Z*- and *E*-forms of indolinobenzospiropyrans (**1**, see the Supporting Information, Figures S13−S17). In contrast to indolinobenzospiropyrans, which undergo *E*- to *Z*-photoreversion to reach a PSS$_{365\ nm}$, the irreversibility of the isomerization in the protonated *E*- and *Z*-bimerocyanines allows for characterization by ^{1}H NMR spectroscopy at room temperature (Figure S12), in addition to observation of intermediate species.

Upon subsequent ex situ addition of base to the *E,E*-biMCH$_2^{2+}$ form at −30 °C (Figure S15), several species can be observed, among which is the semideprotonated and closed form, i.e., [SP]-[*E*-MCH$^+$], and the SP-[*E*-MC] form (scaled subtraction at Figure S17). The residual *E,E*-biMCH$_2^{2+}$ form and the generated bispiropyran form are also present but do not hinder the assignment to the asymmetric species (Figure S16). These ^{1}H NMR spectroscopic data indicate that although for these steady-state conditions UV−vis absorption spectroscopic data does not allow for all mixed isomers to be discriminated, it is clear that the interaction between the units is sufficiently strong to have a substantial effect on the ^{1}H NMR spectra of each of the individual species (Scheme 6).

Noncommutable Multimode Switching Pathways. The stability of the various isomers indicates that several merocyanine forms should be observed in solution upon switching from the bispiropyran form, thermally, photochemically, and with acid. Compounds **2** and **3** show noncommutable behavior in switching, i.e., differences in the order of pH and photochemical switching steps lead to different outcomes (Scheme 7).

The formation of the species responsible for the absorption bands at 620 and 734 nm from a common (protonated) *E*-isomer can be excluded. The noncommutability is demon-

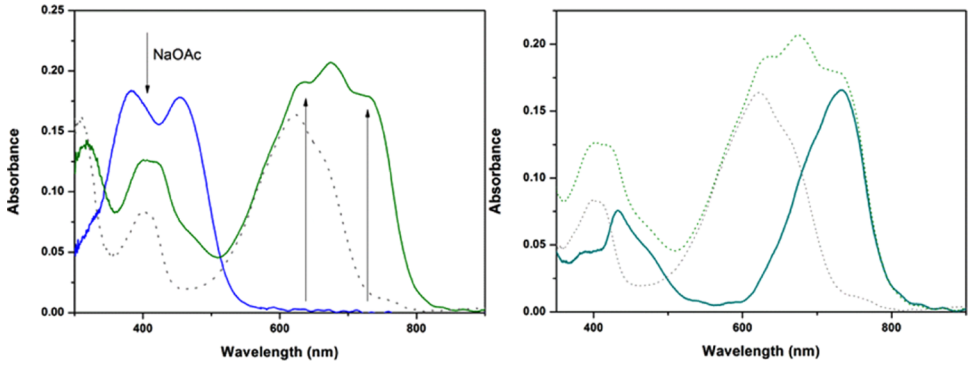

Figure 4. (Top) UV−vis absorption spectrum of *E,E*-biMCH$_2^{2+}$ (blue line) generated by irradiation of **3** (5.7 μM, at −30 °C) in acetonitrile with 5 equiv CF_3SO_3H (green line) after addition of 100 equiv NaOAc (19 μL of a 60 mM 9:1 acetonitrile/water solution). The SP-[*E*-MC] absorption obtained by irradiation (dotted gray line) at −30 °C in the absence of acid is scaled for comparison. (Bottom) The absorption spectrum of the new species with λ_{max} at 734 nm obtained by subtraction of the scaled spectrum of SP-[*E*-MC] (gray dotted line) from the absorption of the mixture of both species (green dotted line). The appearance of the absorption band is not oxygen dependent (Figure S9).

https://dx.doi.org/10.1021/acs.jpca.0c02286
J. Phys. Chem. A 2020, 124, 6458−6467

Scheme 6. Dual Photo- and pH-Switching of 2 and 3 with a Fast Thermal Reversion of the Unprotonated Bimerocyanines, but Full Thermal Stability at Room Temperature in the Protonated States in Addition to Unidirectional Photoisomerization[a]

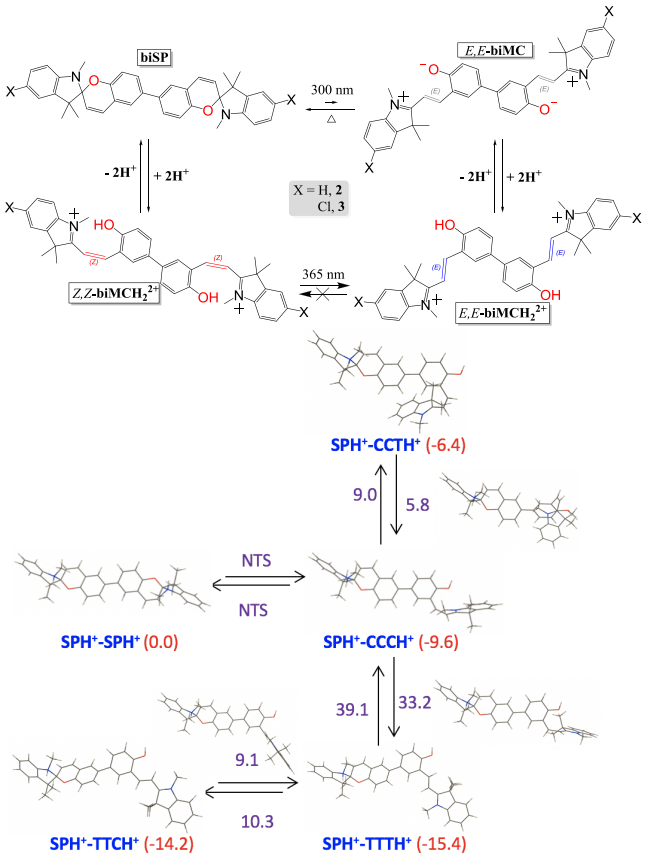

[a]See caption of Figure 1 for more details. NTS means that no transition state could be located, i.e., that the process of opening the SP is (nearly) barrierless.

Scheme 7. Noncommutation in the Photo/Acido/Thermal Switching of 2 and 3

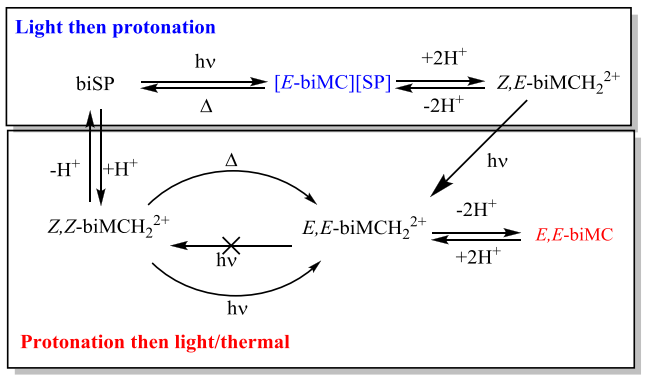

strated as follows. Irradiation of **2** at −30 °C to its $PSS_{300\ nm}$ results in the appearance of the absorption band at 620 nm only (Figure 1). Addition of acid yields *Z,E*-biMCH$_2^{2+}$. After standing in the dark for 30 min at −30 °C, subsequent deprotonation also recovers the absorption at 620 nm only (Figure S18). In contrast, irradiation of *Z,E*-biMCH$_2^{2+}$ at 365 nm (to form *E,E*-biMCH$_2^{2+}$) followed by deprotonation yields the same mixed spectrum upon deprotonation as obtained by irradiation of *Z,Z*-biMCH$_2^{2+}$ at 365 nm.

Thermal Access to the *E,E*-biMC Isomer. The NIR absorption band of the *E,E*-biMC isomer (at 734 nm) cannot be accessed directly through irradiation of the bispiropyran form at any temperature in the absence of acid (Figure S19). It can only be formed by the pH-gated pathway described above (Figures 4 and S10) or by protonation of the *E*-MC-SP intermediate followed by irradiation and deprotonation (Scheme 5). Furthermore, the absorption spectrum generated by protonation of *Z,E*-biMC at −30 °C (PSS_{300}, Figure S20) is identical to an approximately 1:1 mixture of *Z,Z*-biMCH$_2^{2+}$ and the spectrum generated by irradiation of the *Z,Z*-biMCH$_2^{2+}$ form at room temperature in the presence of acid. Hence, the absorption spectra of the protonated *Z,E*- and *E,E*-forms of biMCH$_2^{2+}$ are not distinguishable except by intensity. Notably, if irradiation at 365 nm is limited to below full conversion, then much less of the species absorbing at 734 nm is observed.

At 60 °C, the absorbance at 450 nm increases over time without irradiation indicative of thermal *Z*/*E* isomerization from *Z,Z*-biMCH$_2^{2+}$ to a mixture of *Z,E*-biMCH$_2^{2+}$ and *E,E*-biMCH$_2^{2+}$ (Figure 5, top). Subsequent deprotonation results in the appearance of the absorption band at 734 nm, confirming that the protonated *E,E*-isomer can be accessed thermally also (32 kcal mol^{-1}), and from it the deprotonated *E,E*-isomer (Figure 5, middle).

Summary. The tethering of two spiropyran units via their pyran moiety does not appear to affect significantly photochemical switching from the spiro to the merocyanine forms at low temperature, nor does it affect the protonation-induced ring opening of the spiro unit in comparison with the monospiropyran analogues. However, in contrast to monospiropyrans, protonation yields three thermally stable isomers (*Z,Z*-, *Z,E*-, and *E,E*-) of merocyanine, with the protonated *Z*-bimerocyanine generated initially and the protonated *E*-form formed only after UV irradiation or at elevated temperatures. Furthermore, the photochemically generated protonated *E,E*-isomer of the double spiropyran does not undergo photoreversion to the *Z*-form and is fluorescent. Deprotonation of either *Z,Z*-, *Z,E*-, or *E,E*-isomer results in thermal reversion to recover the bispiropyran form.

The deprotonation yields an isomer (vide supra, Scheme 3) that shows a red-shifted absorption maximum (at 734 nm) consistent with the doubly switched form. The spectral differences between the merocyanine isomers are most probably due to a change in conformation rather than bonding as indicated by the similarities in the coupling constants and chemical shifts in their ^{1}H NMR spectra compared to their monomerocyanine analogue. Additionally, their thermal stability allows for in situ ^{1}H NMR spectroscopic studies, which indicate the presence of intermediate species in several forms. Whereas at room temperature both the *Z*- and *E*-forms of the protonated bimerocyanines are thermally stable, at higher temperatures, e.g., 60 °C, the *Z*-form undergoes thermal isomerization to the *E*-form, specifically to the *Z,E* isomer (which is accessed directly by irradiation of the bispiropyran form) and the *E,E* isomer.

CONCLUSIONS

Increasing the functionality of materials through responsive molecular components can be achieved through the use of so-called multiphotochromes, in which individual units are combined to access additional states and hence properties.

https://dx.doi.org/10.1021/acs.jpca.0c02286
J. Phys. Chem. A 2020, 124, 6458−6467

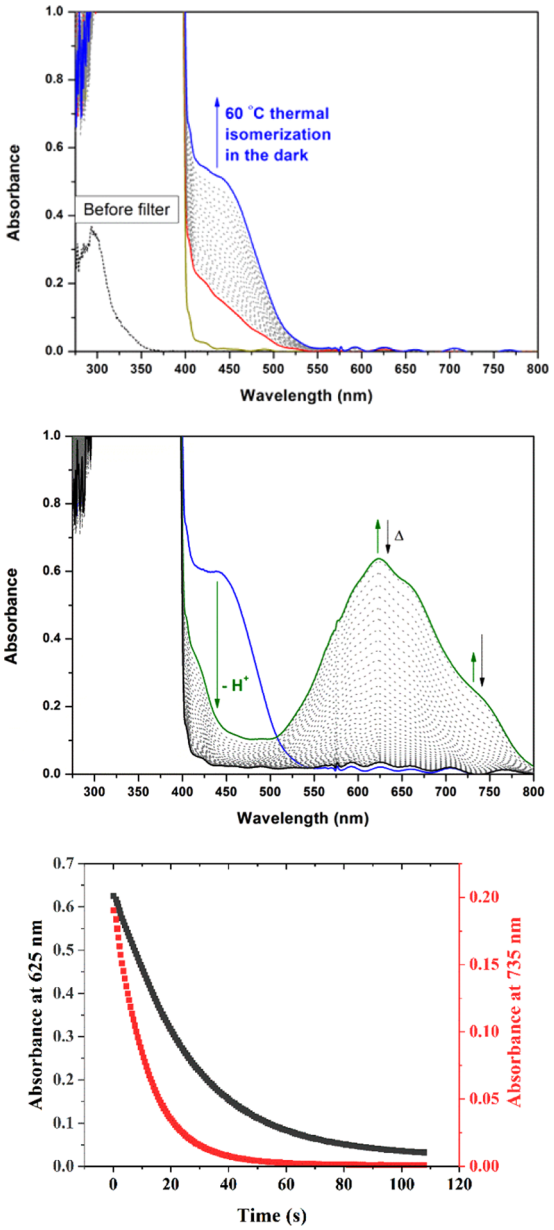

Figure 5. UV−vis absorption spectrum of (top) **2** (18 μM) in acetonitrile before (black dashed line) and after (dark yellow line) placing a 400 nm long-pass filter at the spectrometer light source. 6 equiv CF_3SO_3H was added (red line) and the solution was left in the dark for 47 h at 60 °C, generating SP-[*E*-MC] and *E,E*-biMCH$_2^{2+}$ thermally (blue line). (Middle) Subsequent addition of excess 100 equiv NaOAc in 9:1 acetonitrile/water at 5 °C shows that the NIR-absorbing species had been produced thermally (2 s intervals). The rate of decay (bottom) is consistent with the calculated barriers.

Such complex molecular systems can also present new insight through the stabilization of species not observable in their simpler analogues. In the present case, the coupling of two spiropyrans through their photochromic unit simplifies the pH-gated photochromism of spiropyrans since the protonated *E*- and *Z*-isomers are both thermally stable. Unexpectedly, interactions in the coupled system provide noncommutable access to an otherwise inaccessible *E,E*-merocyanine state, through deprotonation of the *E,E*-biMCH$_2^{2+}$ isomer, formed photochemically or thermally from the *Z,Z*-biMCH$_2^{2+}$ form alone. The large spectral differences between the two species in the deprotonated state, in contrast with their similarity in the protonated state, show how sensitive intramolecular electronic interactions can be to protonation state and allows for the thermal and photochemical behavior of both to be studied providing insights into the reaction dynamics of merocyanines.

■ ASSOCIATED CONTENT

Supporting Information

The Supporting Information is available free of charge at https://pubs.acs.org/doi/10.1021/acs.jpca.0c02286.

Additional ^{1}H NMR; UV−vis absorption and emission spectroscopic data; details of synthesis and characterization (PDF)

■ AUTHOR INFORMATION

Corresponding Authors

Denis Jacquemin − *Université de Nantes, CNRS, CEISAM UMR 6230, F-44000 Nantes, France;* orcid.org/0000-0002-4217-0708; Email: denis.jacquemin@univ-nantes.fr

Wesley R. Browne − *Molecular Inorganic Chemistry, Stratingh Institute for Chemistry, Faculty of Mathematics and Natural Sciences, University of Groningen, 9747 AG Groningen, The Netherlands;* orcid.org/0000-0001-5063-6961; Email: w.r.browne@rug.nl

Authors

Luuk Kortekaas − *Molecular Inorganic Chemistry, Stratingh Institute for Chemistry, Faculty of Mathematics and Natural Sciences, University of Groningen, 9747 AG Groningen, The Netherlands;* orcid.org/0000-0002-3420-4349

Jorn D. Steen − *Molecular Inorganic Chemistry, Stratingh Institute for Chemistry, Faculty of Mathematics and Natural Sciences, University of Groningen, 9747 AG Groningen, The Netherlands*

Daniël R. Duijnstee − *Molecular Inorganic Chemistry, Stratingh Institute for Chemistry, Faculty of Mathematics and Natural Sciences, University of Groningen, 9747 AG Groningen, The Netherlands*

Complete contact information is available at: https://pubs.acs.org/10.1021/acs.jpca.0c02286

Notes

The authors declare no competing financial interest.

■ ACKNOWLEDGMENTS

Financial support was provided by The Netherlands Ministry of Education, Culture and Science (Gravity Program 024.001.035 to W.R.B.). This work used computational resources of the CCIPL center installed in Nantes.

■ REFERENCES

(1) Karimi, M.; Zangabad, P. S.; Baghaee-Ravari, S.; Ghazadeh, M.; Mirshekari, H.; Hamblin, M. R. Smart Nanostructures for Cargo Delivery: Uncaging and Activating by Light. *J. Am. Chem. Soc.* **2017**, *139*, 4584−4610.

(2) Zhang, Y.; Li, Y.; Liu, W. Dipole-Dipole and h-Bonding Interactions Significantly Enhance the Multifaceted Mechanical Properties of Thermoresponsive Shape Memory Hydrogels. *Adv. Funct. Mater.* **2015**, *25*, 471−480.

(3) Chan, B. Q. Y.; Liow, S. S.; Loh, X. J. Organic-Inorganic Shape Memory Thermoplastic Polyurethane Based on Polycaprolactone and Polydimethylsiloxane. *RSC Adv.* **2016**, *6*, 34946−34954.

(4) Luo, Y.; Yu, X. Light and Electrically Responsive Materials Based on Aligned Carbon Nanotubes. *Eur. Polym. J.* **2016**, *82*, 290−299.
(5) Hu, Y.; Lu, C. H.; Guo, W.; Aleman-Garcia, M. A.; Ren, J.; Willner, I. A Shape Memory Acrylamide/DNA Hydrogel Exhibiting Switchable Dual PH-Responsiveness. *Adv. Funct. Mater.* **2015**, *25*, 6867−6874.
(6) Irie, M.; Fukaminato, T.; Matsuda, K.; Kobatake, S. Photochromism of Diarylethene Molecules and Crystals: Memories, Switches, and Actuators. *Chem. Rev.* **2014**, *114*, 12174−12277.
(7) Bandara, H. M. D.; Burdette, S. C. Photoisomerization in Different Classes of Azobenzene. *Chem. Soc. Rev.* **2012**, *41*, 1809−1825.
(8) Dong, M.; Babalhavaeji, A.; Samanta, S.; Beharry, A. A.; Woolley, G. A. Red-Shifting Azobenzene Photoswitches for in Vivo Use. *Acc. Chem. Res.* **2015**, *48*, 2662−2670.
(9) Klajn, R. Spiropyran-Based Dynamic Materials. *Chem. Soc. Rev.* **2014**, *43*, 148−184.
(10) Kortekaas, L.; Browne, W. R. The Evolution of Spiropyran: Fundamentals and Progress of an Extraordinarily Versatile Photochrome. *Chem. Soc. Rev.* **2019**, *48*, 3406−3424.
(11) Moncelsi, G.; Ballester, P. Photoswitchable Host-Guest Systems Incorporating Hemithioindigo and Spiropyran Units. *ChemPhotoChem* **2019**, *3*, 304−317.
(12) Li, M.; Zhang, Q.; Zhou, Y. N.; Zhu, S. Let Spiropyran Help Polymers Feel Force! *Prog. Polym. Sci.* **2018**, *79*, 26−39.
(13) Martin, C. J.; Rapenne, G.; Nakashima, T.; Kawai, T. Recent Progress in Development of Photoacid Generators. *J. Photochem. Photobiol., C* **2018**, *34*, 41−51.
(14) Paramonov, S. V.; Lokshin, V.; Fedorova, O. A. Spiropyran, Chromene or Spirooxazine Ligands: Insights into Mutual Relations between Complexing and Photochromic Properties. *J. Photochem. Photobiol., C* **2011**, *12*, 209−236.
(15) Kundu, P. K.; Olsen, G. L.; Kiss, V.; Klajn, R. Nanoporous Frameworks Exhibiting Multiple Stimuli Responsiveness. *Nat. Commun.* **2014**, *5*, No. 3588.
(16) Howlader, P.; Mondal, B.; Purba, P. C.; Zangrando, E.; Mukherjee, P. S. Self-Assembled Pd(II) Barrels as Containers for Transient Merocyanine Form and Reverse Thermochromism of Spiropyran. *J. Am. Chem. Soc.* **2018**, *140*, 7952−7960.
(17) Peterson, G. I.; Larsen, M. B.; Ganter, M. A.; Storti, D. W.; Boydston, A. J. 3D-Printed Mechanochromic Materials. *ACS Appl. Mater. Interfaces* **2015**, *7*, 577−583.
(18) Wu, Z.; Pan, K.; Mo, S.; Wang, B.; Zhao, X.; Yin, M. Tetraphenylethene-Induced Free Volumes for Isomerization of Spiropyran towards Multifunctional Materials in the Solid State. *ACS Appl. Mater. Interfaces* **2018**, *10*, 30879−30886.
(19) Fihey, A.; Perrier, A.; Browne, W. R.; Jacquemin, D. Multiphotochromic Molecular Systems. *Chem. Soc. Rev.* **2015**, *44*, 3719−3759.
(20) Ramamurthy, V.; Schanze, K. S. *Photochemistry of Organic Molecules in Isotropic and Anisotropic Media*; Marcel Dekker, Inc.: New York, 2003.
(21) Hobley, J.; Malatesta, V.; Giroldini, W.; Stringo, W. π-Cloud and Non-Bonding or H-Bond Connectivities in Photochromic Spiropyrans and Their Merocyanines Sensed by ^{13}C Deuterium Isotope Shifts. *Phys. Chem. Chem. Phys.* **2000**, *2*, 53−56.
(22) Hobley, J.; Malatesta, V.; Millini, R.; Montanari, L.; O'Neil Parker, W., Jr. Proton Exchange and Isomerisation Reactions of Photochromic and Reverse Photochromic Spiro-Pyrans and Their Merocyanine Forms. *Phys. Chem. Chem. Phys.* **1999**, *1*, 3259−3267.
(23) Kortekaas, L.; Chen, J.; Jacquemin, D.; Browne, W. R. Proton Stabilized Photochemically Reversible E/Z Isomerization of Spiropyrans. *J. Phys. Chem. B* **2018**, *122*, 6423−6430.
(24) Hirshberg, Y.; Fischer, E. Multiple Reversible Color Changes Initiated by Irradiation at Low Temperature. *J. Chem. Phys.* **1953**, *21*, 1619.
(25) Feringa, B. L.; Browne, W. R. *Molecular Switches*; Wiley-VCH Verlag GmbH & Co. KGaA: Weinheim, Germany, 2011.
(26) Turro, N. J.; Ramamurthy, V.; Scaiano, J. C. *Principles of Molecular Photochemistry: An Introduction*; University Science Books: Sausalito, 2009.
(27) Ernsting, N. P.; Arthen-Engeland, T. Photochemical Ring-Opening Reaction of Indolinespiropyrans Studied by Subpicosecond Transient Absorption. *J. Phys. Chem. A.* **1991**, *95*, 5502−5509.
(28) Heiligman-Rim, R.; Hirshberg, Y.; Fischer, E. Photochromism in Spiropyrans. Part IV. 1 Evidence for the Existance of Several Forms of the Colored Modification. *J. Phys. Chem. B.* **1962**, *66*, 2465−2470.
(29) Ernsting, N. P.; Dick, B.; Arthen-Engeland, T. The Primary Photochemical Reaction Step of Unsubstituted Indolino-Spiropyrans. *Pure Appl. Chem.* **1990**, *62*, 1483−1488.
(30) Ernsting, N. P. Transient Optical Absorption Spectroscopy of the Photochemical Spiropyran-Merocyanine Conversion. *Chem. Phys. Lett.* **1989**, *159*, 526−531.
(31) Hobley, J.; Malatesta, V. Energy Barrier to TTC-TTT Isomerisation for the Merocyanine of a Photochromic Spiropyran. *Phys. Chem. Chem. Phys.* **2000**, *2*, 57−59.
(32) Buback, J.; Nuernberger, P.; Kullmann, M.; Langhojer, F.; Schmidt, R.; Würthner, F.; Brixner, T. Ring-Closure and Isomerization Capabilities of Spiropyran-Derived Merocyanine Isomers. *J. Phys. Chem. A* **2011**, *115*, 3924−3935.
(33) Buback, J.; Kullmann, M.; Langhojer, F.; Nuernberger, P.; Schmidt, R.; Wu, F.; Brixner, T. Ultrafast Bidirectional Photoswitching of a Spiropyran. *J. Am. Chem. Soc.* **2010**, *132*, 16510−16519.
(34) Wohl, C. J.; Kuciauskas, D. Excited-State Dynamics of Spiropyran-Derived Merocyanine Isomers. *J. Phys. Chem. B* **2005**, *109*, 22186−22191.
(35) Ruetzel, S.; Diekmann, M.; Nuernberger, P.; Walter, C.; Engels, B.; Brixner, T. Photoisomerization among Ring-Open Merocyanines. I. Reaction Dynamics and Wave-Packet Oscillations Induced by Tunable Femtosecond Pulses. *J. Chem. Phys.* **2014**, *140*, No. 224310.
(36) Areephong, J.; Kudernac, T.; de Jong, J. J. D.; Carroll, G. T.; Pantorott, D.; Hjelm, J.; Browne, W. R.; Feringa, B. L. On/off Photoswitching of the Electropolymerizability of Terthiophenes. *J. Am. Chem. Soc.* **2008**, *130*, 12850−12851.
(37) Wesenhagen, P.; Areephong, J.; Landaluce, T. F.; Heureux, N.; Katsonis, N.; Hjelm, J.; Rudolf, P.; Browne, W. R.; Feringa, B. L. Photochromism and Electrochemistry of a Dithienylcyclopentene Electroactive Polymer. *Langmuir* **2008**, *24*, 6334−6342.
(38) Milder, M. T. W.; Areephong, J.; Feringa, B. L.; Browne, W. R.; Herek, J. L. Photoswitchable Molecular Wires: From a Sexithiophene to a Dithienylethene and Back. *Chem. Phys. Lett.* **2009**, *479*, 137−139.
(39) Kortekaas, L.; Ivashenko, O.; van Herpt, J. T.; Browne, W. R. A Remarkable Multitasking Double Spiropyran: Bidirectional Visible-Light Switching of Polymer-Coated Surfaces with Dual Redox and Proton Gating. *J. Am. Chem. Soc.* **2016**, *138*, 1301−1312.
(40) Qu, D. H.; Wang, Q. C.; Zhang, Q. W.; Ma, X.; Tian, H. Photoresponsive Host-Guest Functional Systems. *Chem. Rev.* **2015**, *115*, 7543−7588.
(41) Kortekaas, L.; Lancia, F.; Steen, J. D.; Browne, W. R. Reversible Charge Trapping in Bis-Carbazole-Diimide Redox Polymers with Complete Luminescence Quenching Enabling Nondestructive Read-Out by Resonance Raman Spectroscopy. *J. Phys. Chem. C* **2017**, *121*, 14688−14702.
(42) Chang, Y. M.; Lee, S. H.; Cho, M. Y.; Yoo, B. W.; Rhee, H. J.; Lee, S. H.; Yoon, C. M. Homocoupling of Aryl Iodides and Bromides Using a Palladium/Indium Bimetallic System. *Synth. Commun.* **2005**, *35*, 1851−1857.
(43) Liu, H.-B.; Wang, M.; Wang, Y.; Wang, L.; Sun, L.-C. Synthesis of Tri-and Disalicylaldehydes and Their Chiral Schiff Base Compounds. *Synth. Commun.* **2010**, *40*, 1074−1081.
(44) Keum, S. R.; Roh, H. J.; Choi, Y. K.; Lim, S. S.; Kim, S. H.; Koh, K. Complete ^{1}H and ^{13}C NMR Spectral Assignment of Symmetric and Asymmetric Bis-Spiropyran Derivatives. *Magn. Reson. Chem.* **2005**, *43*, 873−876.
(45) Lee, S.; Ji, S.; Kang, Y. Synthesis and Characterizations of Bis-Spiropyran Derivatives. *Bull. Korean Chem. Soc.* **2012**, *33*, 3740−3744.

https://dx.doi.org/10.1021/acs.jpca.0c02286
J. Phys. Chem. A 2020, 124, 6458−6467

(46) Keum, S.-R.; Choi, Y.-K.; Kim, S.-H.; Yoon, C.-M. Symmetric and Unsymmetric Indolinobenzospiropyran Dimers: Synthesis and Characterization. *Dyes Pigm.* **1999**, *41*, 41−47.
(47) Hatchard, C. G.; Parker, C. A. A New Sensitive Chemical Actinometer - II. Potassium Ferrioxalate as a Standard Chemical Actinometer. *Proc. R. Soc. London, Ser. A* **1956**, *235*, 518−536.
(48) Frisch, M. J.; Trucks, G. W.; Schlegel, H. B.; Scuseria, G. E.; Robb, M. A.; Cheeseman, J. R.; Scalmani, G.; Barone, V.; Petersson, G. A.; Nakatsuji, H. et al. *G16_C01*; Gaussian Inc.: Wallingford, CT, 2016.
(49) Markworth, P. B.; Adamson, B. D.; Coughlan, N. J. A.; Goerigk, L.; Bieske, E. J. Photoisomerization Action Spectroscopy: Flicking the Protonated Merocyanine−Spiropyran Switch in the Gas Phase. *Phys. Chem. Chem. Phys.* **2015**, *17*, 25676−25688.
(50) Yanai, T.; Tew, D. P.; Handy, N. C. A New Hybrid Exchange−Correlation Functional Using the Coulomb-Attenuating Method (CAM-B3LYP). *Chem. Phys. Lett.* **2004**, *393*, 51−57.
(51) Day, J. H. Thermochromism. *Chem. Rev.* **1963**, *63*, 65−80.
(52) Mustafa, A. The Chemistry of Spiropyrans. *Chem. Rev.* **1948**, *43*, 509−523.
(53) Schmidt, S. B.; Kempe, F.; Brügner, O.; Walter, M.; Sommer, M. Alkyl-Substituted Spiropyrans: Electronic Effects, Model Compounds and Synthesis of Aliphatic Main-Chain Copolymers. *Polym. Chem.* **2017**, *8*, 5407−5414.
(54) Shimizu, I.; Kokado, H.; Inoue, E. Photoreversible Photographic System VI. Reverse Photochromism of 1,3,3-Trimethylspiro-[indoline-2,2′-benzopyran]-8′-carboxylic Acid. *Bull. Chem. Soc. Jpn.* **1969**, *42*, 1730−1734.
(55) Roxburgh, C. J.; Sammes, P. G. On the Acid Catalysed Isomerisation of Some Substituted Spirobenzopyrans. *Dyes Pigm.* **1995**, *27*, 63−69.
(56) Zhou, J.; Li, Y.; Tang, Y.; Zhao, F.; Song, X.; Li, E. Detailed Investigation on a Negative Photochromic Spiropyran. *J. Photochem. Photobiol., A* **1995**, *90*, 117−123.
(57) Shiozaki, H. Molecular Orbital Calculations for Acid Induced Ring Opening Reaction of Spiropyran. *Dyes Pigm.* **1997**, *33*, 229−237.
(58) Fissi, A.; Pieroni, O.; Angelini, N.; Lenci, F. Photoresponsive Polypeptides. Photochromic and Conformational Behavior of Spiropyran-Containing Poly(1-Glutamate)s under Acid Conditions. *Macromolecules* **1999**, *32*, 7116−7121.
(59) Wojtyk, J. T. C.; Wasey, A.; Xiao, N. N.; Kazmaier, P. M.; Hoz, S.; Yu, C.; Lemieux, R. P.; Buncel, E. Elucidating the Mechanisms of Acidochromic Spiropyran-Merocyanine Interconversion. *J. Phys. Chem. A* **2007**, *111*, 2511−2516.
(60) Nam, Y.-S.; Yoo, I.; Yarimaga, O.; Park, I. S.; Park, D.-H.; Song, S.; Kim, J.-M.; Lee, C. W. Photochromic Spiropyran-Embedded PDMS for Highly Sensitive and Tunable Optochemical Gas Sensing. *Chem. Commun.* **2014**, *50*, 4251−4254.
(61) Genovese, M. E.; Athanassiou, A.; Fragouli, D. Photoactivated Acidochromic Elastomeric Films for on Demand Acidic Vapor Sensing. *J. Mater. Chem. A* **2015**, *3*, 22441−22447.
(62) Remon, P.; Li, S. M.; Grotli, M.; Pischel, U.; Andreasson, J. An Acido- and Photochromic Molecular Device That Mimics Triode Action. *Chem. Commun.* **2016**, *52*, 4659−4662.
(63) Krongauz, V. A.; Goldburt, E. S. Quasi-Crystals from Irradiated Photochromic Dyes in an Applied Electric Field. *Nature* **1978**, *271*, 43.
(64) Ruetzel, S.; Kullmann, M.; Buback, J.; Nuernberger, P.; Brixner, T. Tracing the Steps of Photoinduced Chemical Reactions in Organic Molecules by Coherent Two-Dimensional Electronic Spectroscopy Using Triggered Exchange. *Phys. Rev. Lett.* **2013**, *110*, No. 148305.
(65) Kullmann, M.; Ruetzel, S.; Buback, J.; Nuernberger, P.; Brixner, T. Reaction Dynamics of a Molecular Switch Unveiled by Coherent Two-Dimensional Electronic Spectroscopy. *J. Am. Chem. Soc.* **2011**, *133*, 13074−13080.
(66) Buback, J.; Nuernberger, P.; Kullmann, M.; Langhojer, F.; Schmidt, R.; Würthner, F.; Brixner, T. Ring-Closure and Isomerization Capabilities of Spiropyran-Derived Merocyanine Isomers. *J. Phys. Chem. A* **2011**, *115*, 3924−3935.
(67) Turro, N. J. *Modern Molecular Photochemistry*; University Science Books: Sausalito, 1991.

https://dx.doi.org/10.1021/acs.jpca.0c02286
J. Phys. Chem. A 2020, 124, 6458−6467